Design and Analysis of Vibration Based MEMS Energy Harvester for Precision Agriculture

H. Aris[1,2,a], D. Fitrio[1,b], J. Singh[1,c]

[1]Centre for Technology Infusion, La Trobe University, 3086, Victoria, Australia.
[2]School of Microelectronic Engineering, Universiti Malaysia Perlis, 02600, Perlis, Malaysia.
[a]haris@students.latrobe.edu.au,[b]d.fitrio@latrobe.edu.au,[c]j.singh@latrobe.edu.au

ABSTRACT

This paper discusses the performances of different cantilever geometry of piezoelectric MEMS Energy Harvester. Resonant frequency, tip deflection, output voltage and peak power response of five different geometries are compared and analysed. Two piezoelectric materials, ZnO and AlN are utilized as part of the cantilever structures. The design and optimization procedures are done using Coventorware®. Meshing refinement study is also carried out to ensure the numerical accuracy of the results and reduce simulation time. The third cantilever design achieved the least resonant frequency, 3.7 kHz and with total peak power response of 0.14 pW.

Keywords: energy harvester, piezoelectric, resonant frequency, tip deflection, peak power response, meshing

1 INTRODUCTION

The steadily decreased in electronic devices sizes and masses over the past few decades have contributed to the development of low power electronic devices. As a result, power harvesting technology based on environmental energy sources has received much attention to replace the conventional batteries. Energy harvesting methods were previously believed to be unreliable due to its low power generation. However, recent electronic devices with low power consumptions which is in the ranges of microwatts and global interest in the green technology have change the trend.

The most popular environmental energy sources are vibration, thermal, solar and radio frequency (RF) and methods to harvest these green sources are through piezoelectric, electromagnetic and electrostatic elements.

With current capabilities of the existing MEMS energy scavenger, most of researchers are still focusing to increase the power density of energy harvester. The development and utilization of different structural materials, optimization of the cantilever geometry and power harvesting circuit are the most commonly methods used to increase the power density.

Vibration from almost all sources as reported by Roundy [1] is between 70 – 125 Hz and worked excellently with piezoelectric based energy harvester. The most popular piezoelectric materials used by researchers are Lead Zirconate Titanate (PZT) [2-5], Zinc Oxide (ZnO) [6], and Aluminium Nitrate (AlN)[7].

2 THEORETICAL CONSIDERATION

A MEMS energy scavenger with cantilever structure works when the cantilever is excited to its resonance frequency and started to displace from initial position. Kinetic energy from cantilever movement can be conserved into electrical power based on linear system theory. Generic model of vibration energy harvester is shown in Fig. 1.

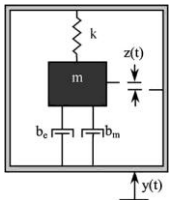

Figure 1: Generic model of vibration energy harvester [8]

The conversion of mechanical energy into electrical energy damps by the mass is depicted as b_e, while mechanical damping is depicted by b_m. The mass in Figure 1 can be translated linearly into equivalent electrical circuit as inductor, spring as inverted capacitor and both mechanical and electrical dampings as resistor. Generic model in Figure 1 can be expressed as a second order differential equation as shown in Equation 1 [8].

$$m\ddot{z} + (b_e + b_m)\dot{z} + kz = -m\ddot{y} \quad (1)$$

where z is spring deflection, y is input displacement, m is mass, b_e is electrical induced damping coefficient, b_m is mechanical damping coefficient and k is spring constant.

Spring constant in the cantilever beam can be calculated with Equation 2, where the maximum displacement for fixed-free beam, x is given by Equation 3.

$$k = \frac{F}{x} \quad (2)$$

$$x = \frac{Fl^3}{3EI} \quad (3)$$

where, F in both Equations 2 and 3 are pointed loading forces, E is the Young's modulus of the beam material and I is the moment of inertia with respect to the neutral axis. If the cantilever bends in the direction of the thickness, moment of inertia I is given by $I = \frac{wt^3}{12}$. Since the generic model of vibration energy harvester as shown in Figure 1 is apparently the simplest case of mechanical resonant system, the resonant frequency can be determined by Equation 4.

$$f = \frac{1}{2\pi}\sqrt{\frac{k}{m}} \quad (4)$$

Mass, m of the system is the accumulation mass of both polysilicon substrate and piezoelectric material.

The stress along the piezoelectric is actually not uniform and changes with the position, but with assumptions that the longitudinal stress is constant, the maximum stress induced along the longitudinal direction of the cantilever is given by Equation 5.

$$\sigma_{1,max} = \frac{Mt}{2I} = \frac{Flt_{beam}}{2I_{beam}} \quad (5)$$

The output electric polarization in the direction of axis-3 is given by Equation 6 and the overall output voltage equation is then given by Equation 7.

$$D_3 = d_{31}\sigma_{1,max} \quad (6)$$

$$V = E_3 t_{piezo} = \frac{D_3 t_{piezo}}{\varepsilon} = \frac{d_{31} Flt_{beam} t_{piezo}}{2I_{beam}\varepsilon} \quad (7)$$

with t_{piezo} is the thickness of piezoelectric material.

3 GEOMETRIC MODEL OF CANTILEVER

Parameters of the cantilevered piezoelectric unimorph in this work are shown in Table 1. Polysilicon is used as a substrate for all models, ZnO as piezoelectric material for Design #1-5 and AlN is used as a piezoelectric material for Design #6. The modal damping used for the simulation is ζ_1=0.010 with base acceleration of 1 m/s^2.

Parameter	Substrate, PolySi	ZnO	AlN
Length of the beam (μm)	4000	4000	4000
Width of the beam (μm)	1000	1000	1000
Thickness (μm)	500	50	50
Young's Modulus (Gpa)	160	129	331
Mass density (kg/m^3)	2230	5680	3200
Piezoelectric coefficient (pC/N)	NA	5.43	2
Poisson ratio	0.22	0.349	0.23

Table 1:Parameters of cantilevered piezoelectric unimorph

The boundary condition for the beams is fixed-free with the free tip capable of moving in a direction normal to the substrate. The other end will be fixed and attached to the substrate. Fig. 2 illustrates the geometric model of the cantilever beams.

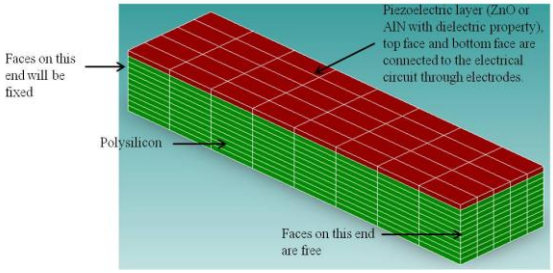

Figure 2: Geometric model of the cantilever

Table 2 and 3 show piezoelectric-strain coefficients and relative permittivity for ZnO and AlN respectively.

D1	0.000e+0	0.000e+0	-5.430e-6
D2	0.000e+0	0.000e+0	-5.430e-6
D3	0.000e+0	0.000e+0	1.167e-5
D4	0.000e+0	0.000e+0	0.000e+0
D5	-1.134e-5	0.000e+0	0.000e+0
D6	0.000e+0	-1.134e-5	0.000e+0
Dielectric	8.55e+00	8.55e+00	1.02e+01

Table 2: Piezoelectric-strain coefficients and relative permittivity for ZnO

D1	000e+0	000e+0	-2.560e-6
D2	000e+0	000e+0	-2.560e-6
D3	000e+0	000e+0	5.53e-6
D4	000e+0	000e+0	000e+0
D5	-4.070e-6	000e+0	000e+0
D6	000e+0	-4.070e-6	000e+0
Dielectric	9.030e+0	9.030e+0	1.073e+1

Table 3: Piezoelectric-strain coefficients and relative permittivity for AlN

4 3D MESHED MODEL

The 3D meshed model of cantilever is generated using Parabolic Manhattan bricks with sizes of 500 μm in the x-axis, 200 μm in the y-axis and 50 μm in the z-axis. Fig. 3 shows all the 3D meshed model of piezoelectric energy harvester generated with the respective mesh settings.

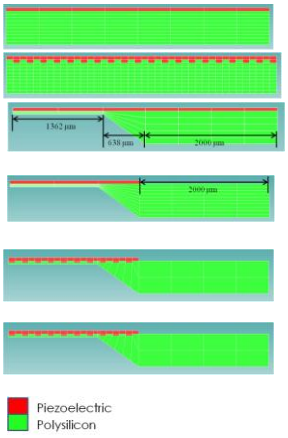

Design 1: ZnO is perpendicularly deposited on top of the substrate.
Design 2: Interdigitated ZnO is deposited on top of the substrate.
Design 3: ZnO is perpendicularly deposited on top of partially etched substrate.
Design 4: Partially etched ZnO is deposited on top of partially etched substrate.
Design 5: Partially etched interdigitated ZnO is deposited on top of partially etched substrate.
Design 6: Partially etched interdigitated AlN is deposited on top of partially etched substrate.

Figure 3: 3D model of the simulated energy harvester

5 SIMULATION RESULTS

5.1 Natural Frequency

Natural frequency of the cantilever occurred at which there is maximum tip displacement in z-axis. Table 4 shows a comparison of the natural frequencies of the first mode for the modelled cantilevers. It can be clearly seen that some of the resonant frequency (Design #2, 4, 5 and 6) increases in the open circuit and it is basically happened due to the stiffening effect of the beam.

Design #	Resonant frequency (kHz) for short circuit	Resonant frequency (kHz) for open circuit
1	43.00	43.00
2	41.20	41.30
3	3.70	3.70
4	4.11	4.14
5	4.02	4.04
6	5.06	5.07

Table 4: Natural frequencies of the first cantilever mode for open and short circuits

5.2 Misses Stress Distribution Analysis

With the direct effect of piezoelectricity, piezoelectric materials will generate an electric charge (or voltage) when they are under mechanical stress. Therefore, misses stress distribution analysis is essential to determine the magnitude of voltage that can be generated by cantilever. Fig. 4 shows the misses stress distribution for the first cantilever mode.

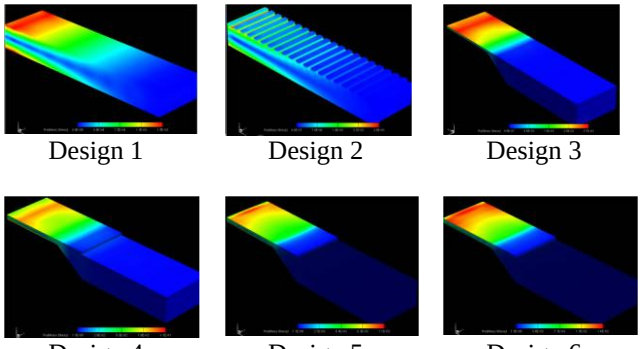

Design 1 Design 2 Design 3

Design 4 Design 5 Design 6

Figure 4: Misses stress distribution for the first cantilever mode

As can be observed from Figure 6, Design 2 resulted in the highest max-value of misses stress, 2.8e-3 MPa but with a quite high resonant frequency, 41.3 kHz while at the same time Design 3 is capable to achieve max-value of misses stress of 2.7e-3 MPa at 4.14 kHz.

5.3 Tip Displacement Analysis

Cantilever tip diflections is caused by the base excitation, 1 m/s^2. Fig. 5 shows the deflection when the cantilever at the short circuit condition, and achieved the highest value of 0.253 µm with Design 3.

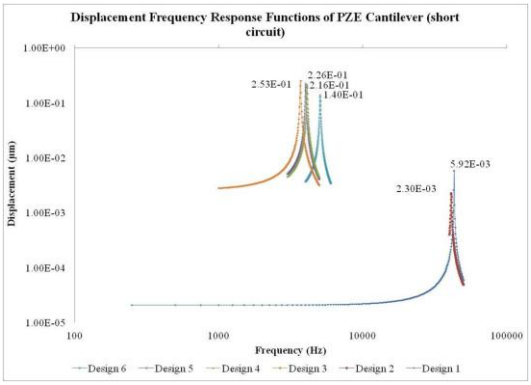

Figure 5: Tip deflection of cantilevers in short circuit conditions

Fig. 6 shows the deflection of cantilever when applied with resistive load and reached open circuit condition. As expected, the highest value of 0.245 µm is achieved with Design 3.

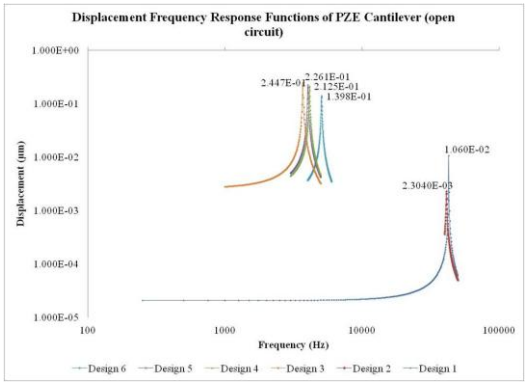

Figure 6: Tip deflection of cantilevers in open circuit conditions

5.4 Output Voltage Analysis

As per output voltage analysis, it is not reflected by the maximum tip deflection value of cantilever. Output voltage value is measured across the cantilever and as shown in Fig. 7, the highest value of output voltage 33.51 µV is achieved by Design 1. However, this design is impractical to be used to harvest energy from agricultural environment due to its high resonant frequency. Design 3 resulted in output voltage of 3.72 µV when 100 ohm resistive load is applied to the cantilever and achieved at 10 times smaller resonant frequency compared to Design 1.

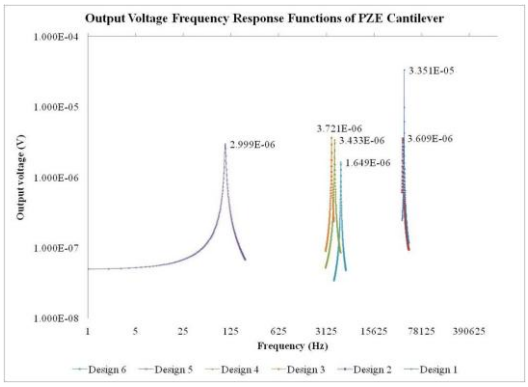

Figure 7: Output voltage frequency response of the cantilevers

5.5 Peak Power Response Analysis

By attaching a 100 Ω resistive load to the piezoelectric energy harvester, the output power as shown in Fig. 8 has been extracted from the cantilever beam. Design 1 has scavenged as high as 11.23 pW and followed by Design 3 with 0.14 pW. Due to low piezoelectric coefficient in AlN, Design 6 has produced only 0.03 pW of power output compared to ZnO in Design 5 with exactly the same geometrical shape and size.

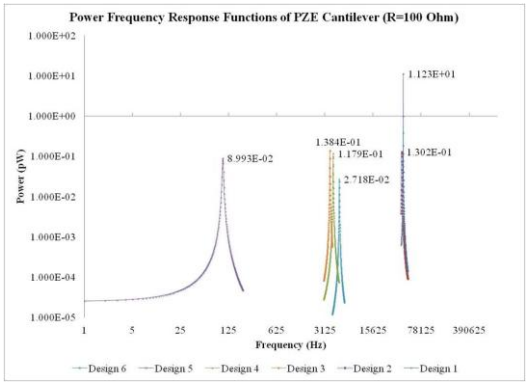

Figure 8: Power frequency response of the PZE cantilever

6 CONCLUSION

Six designs of MEMS piezoelectric energy harvester have been designed and simulated with Coventorware®. A variety of methods have been used to properly place piezeoelectric layer in order to obtain the highest output power. Two types of piezoelectric material, ZnO and AlN have been used in this study where it can be clearly seen that ZnO shows better achievement compared to AlN. Table 5 shows the performance comparisons of the designed MEMS PZE energy harvester.

Design #	Resonant frequency (kHz) for short circuit	Resonant frequency (kHz) for open circuit	Max-displacement (µm)	Output voltage (µV)-with 100 ohms resistive load	Peak power response (pW) – with 100 ohms resistive load
1	43.00	43.00	0.011	33.51	11.23
2	41.20	41.30	0.002	3.61	0.13
3	3.70	3.70	0.245	3.72	0.14
4	4.11	4.14	0.032	3.43	0.12
5	4.02	4.04	0.226	3.00	0.09
6	5.06	5.07	0.140	1.65	0.03

Table 5: Performance comparisons of the designed MEMS PZE energy harvesters

REFERENCES

[1] S. J. Roundy, "Energy Scavenging for Wireless Sensor Nodes with a Focus on Vibration to Electricity Conversion," Doctor of Philosophy in Engineering-Mechanical Engineering, Mechanical Engineering, The University of California, Berkeley, California, 2003.

[2] Y. B. Jeon, R. Sood, J. H. Jeong, and S. G. Kim, "MEMS power generator with transverse mode thin film PZT," *Sensors and Actuators a-Physical*, vol. 122, pp. 16-22, Jul 29 2005.

[3] H.-B. Fang, J.-Q. Liu, Z.-Y. Xu, L. Dong, L. Wang, D. Chen, B.-C. Cai, and Y. Liu, "Fabrication and performance of MEMS-based piezoelectric power generator for vibration energy harvesting," *Microelectronics Journal*, vol. 37, pp. 1280-1284, 2006.

[4] J.-Q. Liu, H.-B. Fang, Z.-Y. Xu, X.-H. Mao, X.-C. Shen, D. Chen, H. Liao, and B.-C. Cai, "A MEMS-based piezoelectric power generator array for vibration energy harvesting," *Microelectronics Journal*, vol. 39, pp. 802-806, 2008.

[5] B. S. Lee, S. C. Lin, W. J. Wu, X. Y. Wang, P. Z. Chang, and C. K. Lee, "Piezoelectric MEMS generators fabricated with an aerosol deposition PZT thin film," *J. Micromech. Microeng.* , vol. 19, p. 8, 2009.

[6] W.-Y. Chang, T.-H. Fang, Cheng-IWeng, and S.-S. Yang, "Flexible piezoelectric harvesting based on epitaxial growth of ZnO," *Appl Phys A : Materials Science and Processing*, vol. 102, p. 7, 2011.

[7] R. Elfrink, T. M. Kamel, M. Goedbloed, S. Matova, D. Hohlfeld, Y. v. Andel, and R. v. Schaijk, "Vibration energy harvesting with aluminum nitride-based piezoelectric devices," *J. Micromech. Microeng.*, vol. 19, p. 8, 2009.

[8] S. Roundy, P. K. Wright, and J. Rabaey, "A study of low level vibrations as a power source for wireless sensor nodes," *Computer Communications*, vol. 26, pp. 1131-1144, 2003.